

Is cell ratio important in deep learning? A robust comparison of deep learning methods for multi-scale cytopathology cell image classification: from convolutional neural networks to visual transformers.

Wanli Liu^a, Chen Li^{a,*}, Md Mamunur Rahaman^a, Hongzan Sun^b, Xiangchen Wu^c, Weiming Hu^a, Haoyuan Chen^a, Changhao Sun^a, Yudong Yao^d, Marcin Grzegorzec^e

^a*Microscopic Image and Medical Image Analysis Group, MBIE College, Northeastern University, 110169, Shenyang, PR China*

^b*China Medical University, 110001, Shenyang, PR China*

^c*Suzhou Ruiguan Technology Company Ltd., Suzhou 215000, China*

^d*Department of Electrical and Computer Engineering, Stevens Institute of Technology, Hoboken, NJ 07030, USA*

^e*University of Lübeck, Germany*

Abstract

Cervical cancer is a very common and fatal cancer in women. Cytopathology images are often used to screen this cancer. Since there is a possibility of a large number of errors in manual screening, the computer-aided diagnosis system based on deep learning is developed. The deep learning methods required a fixed size of input images, but the sizes of the clinical medical images are inconsistent. The internal cell ratios of the images are suffered while resizing it directly. Clinically, the ratios of cells inside cytopathological images provide important information for doctors to diagnose cancer. Therefore, it is illogical to resize directly. However, many existing studies resized the images directly and obtained very robust classification results. To find a reasonable interpretation, we have conducted a series of comparative experiments. First, the raw data of the SIPaKMeD dataset are preprocessed to obtain the standard and scaled datasets. Then, the datasets are resized to 224×224 pixels. Finally, twenty-two deep learning models are used to classify standard and scaled datasets. The conclusion is that the deep learning models are robust to changes in the internal cell ratio of cervical cytopathological images. This conclusion is also validated on the Herlev dataset.

Keywords: Cervical cancer, Deep learning, Pap smear, Cell ratio, Visual Transformer, Robustness comparison

1. Introduction

Cancer is an extremely deadly disease. Approximately 9.6 million people die from cancer every year [1]. According to the latest world cancer statistics, cervical cancer is the seventh most common cancer globally and ranks fourth in the incidence of women. In developing and low-income countries, the mortality rate due to cervical cancer is very high because these women have less hygiene knowledge and access to medical facilities [2]. These situations occur because these women lack hygiene knowledge

and the medical security conditions in these countries are not very good. Human papillomavirus (HPV) is the leading cause of cervical cancer [3].

HPV is the most common sexually transmitted virus in the world [4]. There are about 200 types of HPV viruses are discovered so far, among them 13 are high-risk types. 70% of all cervical cancers are caused by HPV type 16 and 18 [5, 6]. 24% of women are detected to be infected with HPV type 16, and 9% of women are infected with HPV type 18 [5, 7, 8]. Most of the causes of cervical cancer are premature sexual intercourse, intercourse with multiple partners, early pregnancy, weak immune system, smoking, having oral contraceptives and improper menstrual hygiene. Common symp-

*Corresponding author

Email address: lichen201096@hotmail.com (Chen Li)

toms related to cervical cancer are abnormal vaginal bleeding, vaginal discharge, and moderate pain during sexual intercourse [9]. Cervical cancer can be prevented if detected early and facilitates appropriate treatment [10].

Cervical cytopathology is usually used to diagnose cervical malignancies. Because the cervical cytopathological examination cost is relatively low, it is convenient for general investigation [10, 11]. The traditional detection process is to collect cells from the patient’s cervical squamous column with a brush or spatula, and then smear the cells on a glass slide. A professional pathologist observes it under a microscope and determines whether there is any malignancy or not. However, manual screenings are troublesome, time-consuming, and prone to artificial errors because thousands of cells are in different orientations and superimposed on each slide [12]. This problem needs a solution urgently.

In order to solve the problems with manual screening, an automatic computer-aided diagnosis system (CAD) has been proposed widely to analyze the pap slices rapidly and accurately. In addition, the computerized system can also process a large number of images, which provides convenience for clinical follow-up, comparative research and personalized medicine [13]. Nowadays, deep learning techniques are widely used in computer vision, medical imaging, natural language processing and other fields [14, 15]. In traditional CAD systems, the main limitation is that the features are manually extracted, which cannot guarantee the classification results optimality. However, the deep learning technique is an end-to-end method that can automatically learn features [16]. The performance of deep learning technology in image analysis is better than traditional machine learning-based methods. However, training a deep learning model requires a considerable number of labeled data sets [17]. A key question about deep learning is that although it provides excellent results, its characteristics are incomprehensible to humans [18].

The deep learning programs currently used in the field of medical image analysis are all proven and most efficient algorithms. Convolutional Neural Network (CNN) is a trendy deep architecture. It is widely used in image segmentation and classification [14]. A CNN model classifies normal cells and abnormal cells in the cell classification task by extracting hierarchical features from the original image [19]. Recently, a Visual Transformer (VT) that

applies the Transformer architecture for processing Natural Language Processing (NLP) tasks to the field of computer vision. There is a VT model called ViT, which has better results than the latest convolutional network under the premise of pre-training with a large amount of data, and the computing resources required for training are greatly reduced. Nevertheless, when the amount of data is small, the effect may not be ideal [20].

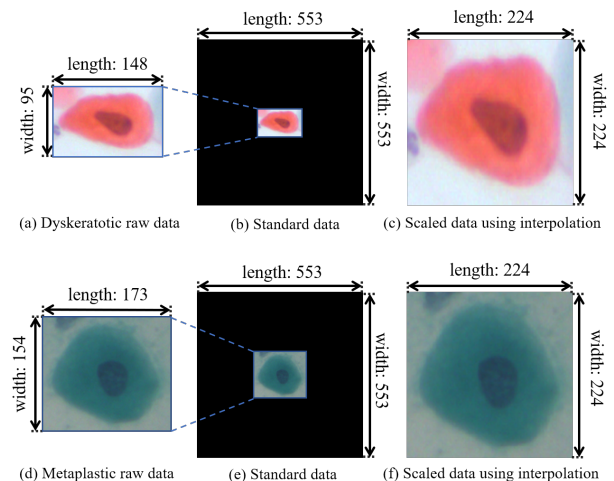


Figure 1: Visual comparisons among raw data, standard data and scaled data.

The input of the deep learning models are consistent, but the size of clinical cervical cell images are mostly inconsistent. The internal cell ratio informations are lost after resizing the images directly. A comparison of raw data, standard data and scaled data using interpolation is shown in Fig. 1. The scaled data is obtained after resizing the raw data to 224×224 pixels. It can be seen that as a result of scaling up the dyskeratotic raw data, the aspect ratio is from $148 : 95$ to $224 : 224$, which changes a lot. Moreover, the cell morphology and cell ratio which means the ratio between cytoplasm and nucleus are also lost. However, the cell morphology and cell ratio in cytopathological images provide important information for doctors to diagnose cancer clinically [21]. According to the standard data in the figure, it can be seen that in the process of standardizing the dyskeratotic raw data, these important information are not lost. Moreover, the resulted scaled data in dyskeratotic class and metaplastic class become very similar after resizing directly, which contradicts the clinical explanations. Therefore, it is illogical to resize directly. How-

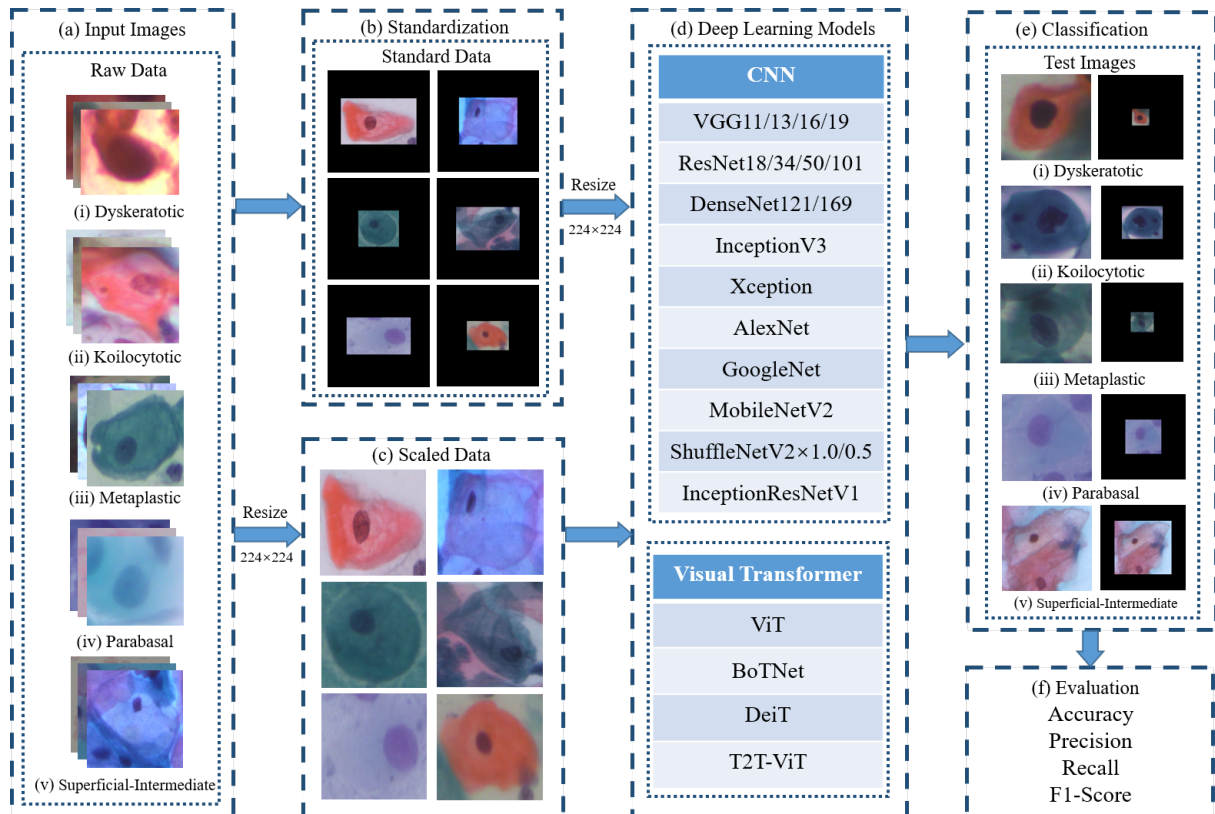


Figure 2: Workflow of a robustness comparison of deep learning methods for multiscale cell image classification.

ever, most existing studies directly resize the cell images, and their results are still robust. In order to find a reasonable explanation, this paper proposes a robust comparison of deep learning methods for multi-scale cell image classification tasks.

In this paper, an experimental platform for the robustness comparison of deep learning methods in multi-scale cell image classification tasks is developed. The workflow diagram of the proposed method is shown in Fig. 2. First of all, the raw data from the SIPaKMeD public dataset, consisting of 4049 cell images, are used in this paper [22]. Secondly, the raw data are standardized and resized directly to get the standard and scaled data, respectively. Thirdly, the scaled and standard data are resized to 224×224 pixels and used as training samples. Finally, the unseen test images are fed into the models for classification. The performance is evaluated by calculating the accuracy, precision, recall and F1-Score on the validation and test sets.

In addition, 22 well-known deep learning models are selected in this experiment. Eighteen of them are CNNs, including VGG11 [23],

VGG13 [23], VGG16 [23], VGG19 [23], ResNet18 [24], ResNet34 [24], ResNet50 [24], ResNet101 [24], DenseNet121 [25], DenseNet169 [25], InceptionV3 [26], Xception [27], AlexNet [28], GoogLeNet [29], MobileNetV2 [30], ShuffleNetV2x1.0 [31], ShuffleNetV2x0.5 [31], InceptionResNetV1 [32]. The remaining four models are VTs, including ViT [20], BoTNet [33], DeiT [34], T2T-ViT [35].

The structure of this paper is as follows: Sec. 2 elaborates the related work of deep learning for the classification of cervical cells. Sec. 3 describes the datasets, data preprocessing methods, and deep learning models. Sec. 4 explains the results of the comparative experiment and the analysis of the experimental results, including the experimental settings and evaluation indicators. Sec. 5 summarizes this paper and proposes the future work direction.

2. Related work

In this section, the related work of deep learning in cervical cell image classification tasks is briefly

introduced. For more detailed information, please refer to our review paper [13].

In [36], deep learning and transfer learning are applied to the binary classification task of cervical cell images for the first time. This paper uses the Herlev and HEMLBC datasets to evaluate performance. All images are resized to 256×256 pixels. The HEMLBC dataset is a private database containing 2370 cervical cell images. The accuracy on the HEMLBC dataset is 98.6%. And the accuracy on the Herlev data set is 98.3%.

In [37], a model that combines CNN and machine learning to classify cervical cell images is proposed. Among them, the VGG network is used to extract features, and the Support Vector Machine (SVM) is used for classification. This paper uses a private dataset containing 71344 cervical cell images and divides the original cell image into several pieces of 224×224 pixels. F1-Score of the classification result is 78%.

In [38], the paper uses the Herlev dataset, in which 70% of the images are used for training and 30% of the images are used for testing. Images smaller than 227×227 pixels in the dataset are supplemented by blank areas. This work uses the pre-trained AlexNet network for feature extraction, then transfers the features to SVM for two classifications. The accuracy of this method reaches 99.19%.

In [39], VGG16 and ResNet architecture network are used to classify the CerviSCAN and Herlev dataset. CerviSCAN is a private database containing 12043 cervical cell images. In this paper, the input size of the image is resized to 100×100 pixels. The F1-Score on VGGNet is 82%. And the F1-Score on ResNet is 83%.

A cervical cell analysis system for detection, segmentation, and classification is proposed in [40]. This work uses AlexNet for transfer learning to classify the Herlev dataset. They prove that segmentation is not necessarily related to classification. The accuracy of the 2-class classification task and 7-class classification task reaches 99.3% and 93.75%.

A comparative experiment using deep learning to classify cervical cell images is proposed in [41]. This paper compares the performance of ResNet101, DenseNet161, AlexNet, VGG19_bn, and SqueezeNet1.1 on the Herlev dataset. Among them, DenseNet161 performs the best, with accuracy rates of 94.38% and 68.54% on 2-class classification and 7-class classification respectively.

In [42], InceptionV3, ResNet152, and Inception-ResNetV2 are used for feature concatenation and ensemble learning to classify cervical cells. This paper uses the 2D Hela dataset, Pap smear dataset, and Hep-2 cell image dataset for performance evaluation. All images are resized to 256×256 pixels. The comprehensive result of multiple models in this method is better than the result of a single model, and the accuracy rate on the Herlev dataset reaches 93.04%.

In [43], this paper transfers the pre-segmented cervical cell images into a compact version of VGG for classification. This compact version has only 7 layers, which reduces the computational cost. In this paper, the Herlev dataset is used for performance evaluation. The width of the image is resized to 200 pixels and is proportional to the length. The accuracy of the 2-class classification is 98.1%. The accuracy of the 7-class classification is 95.9%.

In [44], a method to directly classify Whole Slide Image (WSI) cervical cell clusters without segmentation is proposed. This paper proposes a feature interpretation method based on principal component analysis to visualize and understand the model. The method is evaluated on the SIPaKMeD and Herlev datasets, and WSI patches and single-cell images are resized to 224×224 and 80×80 pixels. The accuracy of this method is 96.37% on WSI patches and 99.63% on single-cell images.

In [45], an Ensemble Transfer Learning (ETL) framework for classifying cervical histopathological images is proposed. This method develops the transfer learning structures of InceptionV3, Xception, VGG16, and ResNet50. Then an evolutionary learning strategy based on weighted voting is introduced. This method is verified on a dataset composed of 307 images, the image is resized to 299×299 pixels and 224×224 pixels and input to the network. The highest accuracy rate obtained is 98.61%.

In [46], a cell classification algorithm combining InceptionV3 and artificial features is proposed. This method inherits the powerful learning ability of transfer learning to solve the problem of underfitting. This method uses the Herlev dataset to classify cervical cell images. The images of the dataset are filled with zero to maintain the aspect ratio of 1:1, and then they are resized to 299×299 pixels. The accuracy rate of this paper is over 98%.

In [47], a system for cervical cancer detection and classification is proposed. This method uses

an ensemble classifier that combines linear discriminant, SVM, k -nearest neighbor, boosted trees, and bagged trees for classification. In the SIPaKMeD dataset, the accuracy rate of the 2-class classification is 98.27%, and the accuracy rate of the 5-class classification is 94.09%.

In [48], a novel internet of health things (IoHT)-driven deep learning framework for detection and classification of cervical cancer images is proposed. This work uses pre-trained CNN models for feature extraction and machine learning models for classification. The Herlev dataset is used to evaluate performance. With the participation of the random forest classifier, the CNN pre-training model ResNet50 achieves a high accuracy rate of 97.89%.

In [49], a method combining convolutional network and variable autoencoder for cervical cell classification is proposed. The use of a variable autoencoder reduces the dimensionality of the data for further processing with the participation of the Softmax layer. This method uses the Herlev dataset for evaluation, images are resized at different scales to prevent further distortions. This work achieves a maximum accuracy of 99.4%

A cervical cancer cell detection and classification system based on CNNs is proposed in [50]. This method uses the CNN model to extract features and then uses the classifier based on extreme learning machine for classification. The CNN model input is the image of size 224×224 . The Herlev dataset is used to evaluate the performance, and the accuracy rates on 2-class and 7-class classification tasks are 99.5% and 91.2%, respectively.

In [51], a hybrid deep feature fusion method based on deep learning is proposed to accurately classify cervical cells. This paper uses the SIPaKMeD dataset to evaluate the performance of the model. All images are resized to 224×224 pixels. For 2-class, 3-class and 5-class classification tasks, this method obtains accuracy rates of 99.85%, 99.38% and 99.14%, respectively.

In [52], a classification method of cervical cells based on Graph Convolutional Network (GCN) is proposed. This work clusters the CNN features of all cervical cell images to construct a graph structure. Then GCN is applied to generate relation-aware features. GCN features are merged to enhance the distinguishing ability of CNN features. This work proves its feasibility and effectiveness on the SIPaKMeD dataset. Each image of this dataset is resized to 80×80 pixels, with an accuracy rate

of 98.37%.

In [53], an ensemble method using InceptionV3, Xception, and DenseNet169 three pre-trained CNN models for cervical cell image classification is proposed. This method uses classifier fusion based on fuzzy levels. The SIPaKMeD and Mendeley datasets are used for evaluation. The accuracy rates of 2-class and 5-class classification tasks on the SIPaKMeD dataset are 98.55% and 95.43%, respectively. The accuracy rate achieved on the Mendeley dataset is 99.23%.

In [54], a new method using transfer learning and progressive resizing technology is proposed. The SIPaKMeD dataset is used for evaluation. This method trains the model iteratively by gradually increasing the image size from 224×224 pixels to 256×256 , 512×512 , and 1024×1024 pixels. The accuracy rate of WSI image multi-classification reaches 99.70%.

In [55], a fully automated framework for cytological image classification is proposed. The framework extracts deep features from CNN models and uses evolutionary optimization algorithms and gray wolf optimizers to select the optimal feature subset. Finally, the SVM classifier is used for classification. Mendeley, Herlev, and SIPaKMeD datasets are used for evaluation, and the classification accuracy rates are 99.47%, 98.32%, and 97.87%, respectively.

3. Materials and methods

3.1. Datasets

3.1.1. SIPaKMeD

A publicly available SIPaKMeD dataset is used to compare the performance of the deep learning models. The database contains 4049 separated cervical cell images, all of which are cropped from clustered cell images obtained by a CCD camera. These images are classified into five categories, dyskeratotic, koilocytotic, metaplastic, parabasal, and superficial intermediate. Some examples of the SIPaKMeD dataset are shown in Fig. 3 [22]. It is seen that the color of the cells in the same category is different. The color information in the cytopathology images are not significant, but it is very important for the histopathology images.

In each category of the dataset, 60% of the data are randomly selected for training, 20% is for validation and the remaining data is for testing. Then, the deep learning models are used to perform the

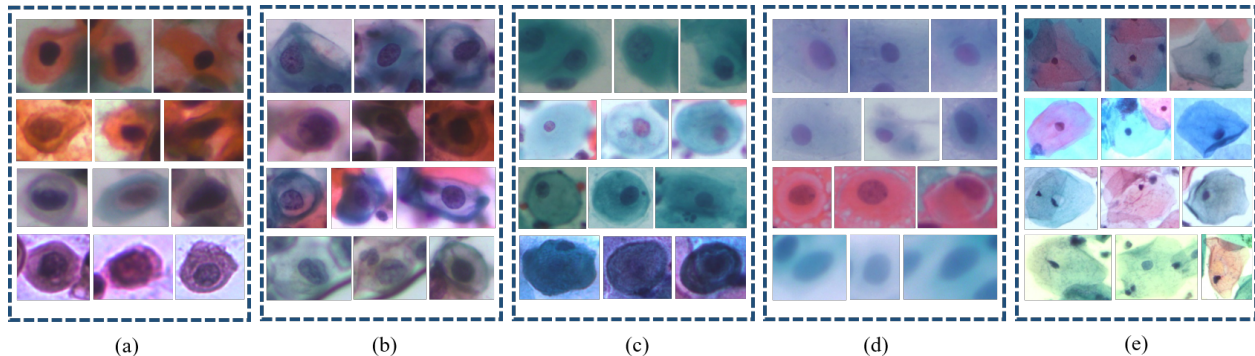


Figure 3: SIPaKMeD dataset example: (a) Dyskeratotic, (b) Koilocytotic, (c) Metaplastic, (d) Parabasal, (e) Superficial-Intermediate.

5-class classification. The training set, validation set, and test set are shown in Table 1.

To further check the model performance, we have performed five-fold cross-validation and showed in the extended experiment 4.4.1.

In the extended experiment 4.4.2, the training and validation set of the SIPaKMeD dataset mentioned above are augmented, and the data increases four times by rotating 180 degrees, flipping left and right, flipping up and down. Then, the augmented data are standardized and resized directly to get the standard and scaled data, respectively. The augmented scaled data and standard data are used to train models. The arrangement of data is shown in Table 1.

Table 1: SIPaKMeD data and augmented data arrangement. (D: Dyskeratotic, K: Koilocytotic, M: Metaplastic, P: Parabasal, S: Superficial-Intermediate. The upper part of the table is the SIPaKMeD data arrangement, and the lower part is the SIPaKMeD augmented data arrangement.)

Data/Class	D	K	M	P	S	Total
Train	488	495	476	473	499	2431
Val	163	165	159	157	166	810
Test	162	165	158	157	166	808
Total	813	825	793	787	831	4049
Train	1952	1980	1904	1892	1996	9724
Val	652	660	636	628	664	3240
Test	162	165	158	157	166	808
Total	2766	2805	2698	2677	2826	13772

3.1.2. Herlev

The Herlev dataset contains 917 cell images, including seven categories: Normal squamous, Intermediate squamous, Columnar, Mild dysplasia,

Moderate dysplasia, Severe dysplasia and Carcinoma *in situ*. Furthermore, these seven categories can also be divided into normal and abnormal types, where the normal type includes Normal squamous, Intermediate squamous, Columnar with 242 images, and the abnormal type includes Carcinoma *in situ*, Mild dysplasia, Moderate dysplasia, Severe dysplasia with 675 images, some examples are shown in Fig. 4 [56].

In the extended experiment 4.4.3, Herlev dataset is used for the two-class classification tasks. In each category of the dataset, 60% of the data are randomly selected for training, 20% of the data for validation, and 20% of the data for testing. Because the amount of data is relatively small, the data increases four times by rotating 180 degrees, flipping left and right, flipping up and down. Then the augmented data are standardized and resized directly to get the standard and scaled data, respectively. The augmented scaled data and standard data are used as the input of models for classification. The augmented data arrangement is shown in Table 2.

Table 2: Herlev augmented data arrangement.

Data/Class	Normal	Abnormal	Total
Train	584	1620	2204
Val	192	540	732
Test	48	135	183
Total	824	2295	3119

3.2. Data preprocessing

The size of cervical cell images in the dataset are inconsistent, but the input required by the deep

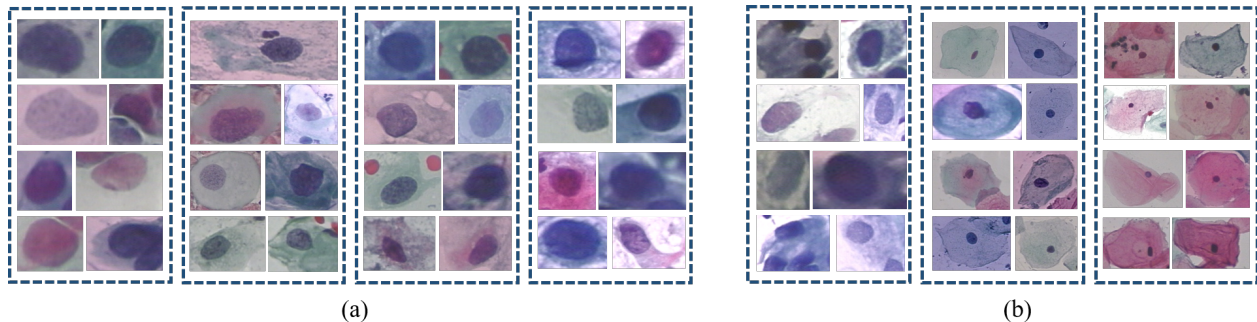


Figure 4: Herlev dataset example: (a) **Abnormal** (From left to right: Carcinoma *in situ*, Mild dysplasia, Moderate dysplasia, Severe dysplasia.), (b) **Normal** (From left to right: Columnar, Intermediate squamous, Normal squamous.).

learning models are consistent. In order to discover whether the ratios of cells in the image impact the performance of the models, MATLAB is used to standardize and centralize the cervical cell images (raw data) in the dataset. The standard operation is to check whether the width of the raw data is longer than the length, if so, rotate the raw data by 90 degrees counterclockwise. Otherwise, no processing is done. The centralization operation is to find the longest side length in all images and then use zero to supplement all images to square matrices of that length. The standardized and centralized images are called the "standard data", some examples are shown in Fig. 5.

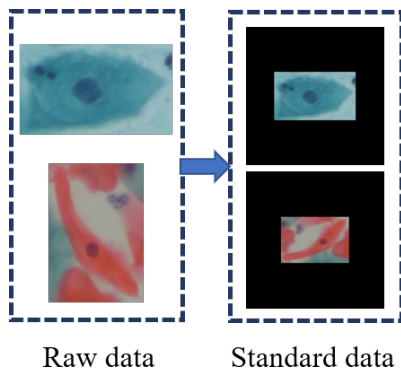


Figure 5: Data preprocessing examples.

3.3. Deep learning models

This robustness comparison experiment uses deep learning models to classify cervical cell images. First, the training and validation sets generated by scaled data and standard data are used to train models. Then, the test set is used to evaluate

the performance of models. The two classification results are compared and analyzed through the obtained evaluation indicators to determine whether the ratio of cells impacts the model performance or not. Twenty-two deep learning models are used in this experiment. Eighteen of the models are CNNs, including VGG11 [23], VGG13 [23], VGG16 [23], VGG19 [23], ResNet18 [24], ResNet34 [24], ResNet50 [24], ResNet101 [24], DenseNet121 [25], DenseNet169 [25], InceptionV3 [26], Xception [27], AlexNet [28], GoogLeNet [29], MobileNetV2 [30], ShuffleNetV2 \times 1.0 [31], ShuffleNetV2 \times 0.5 [31], InceptionResNetV1 [32]. Four of the models are VTs, including ViT [20], BoTNet [33], DeiT [34], T2T-ViT [35].

The references, parameters, the top-1 accuracy on the ImageNet dataset, and major remarks of the 22 models can be seen in the Appendix (Table 12).

In order to know how the CNN models extract features to classify images, we take Xception and InceptionV3 as examples. The input images are scaled data and standard data. Some feature maps extracted from the second convolution block in the networks are shown in Fig. 6.

4. Experiments and analysis

4.1. Experimental setup

This comparative experiment is carried out on a local computer. The running memory of this computer is 32GB. It uses the Win10 Professional operating system and is equipped with an 8GB NVIDIA GeForce RTX 2080 GPU. Python 3.7, Pytorch 1.8.0, and Torchvision 0.9.0 are configured on this computer. For all models, the image input size is $224 \times 224 \times 3$. The learning rate is 0.0002. The

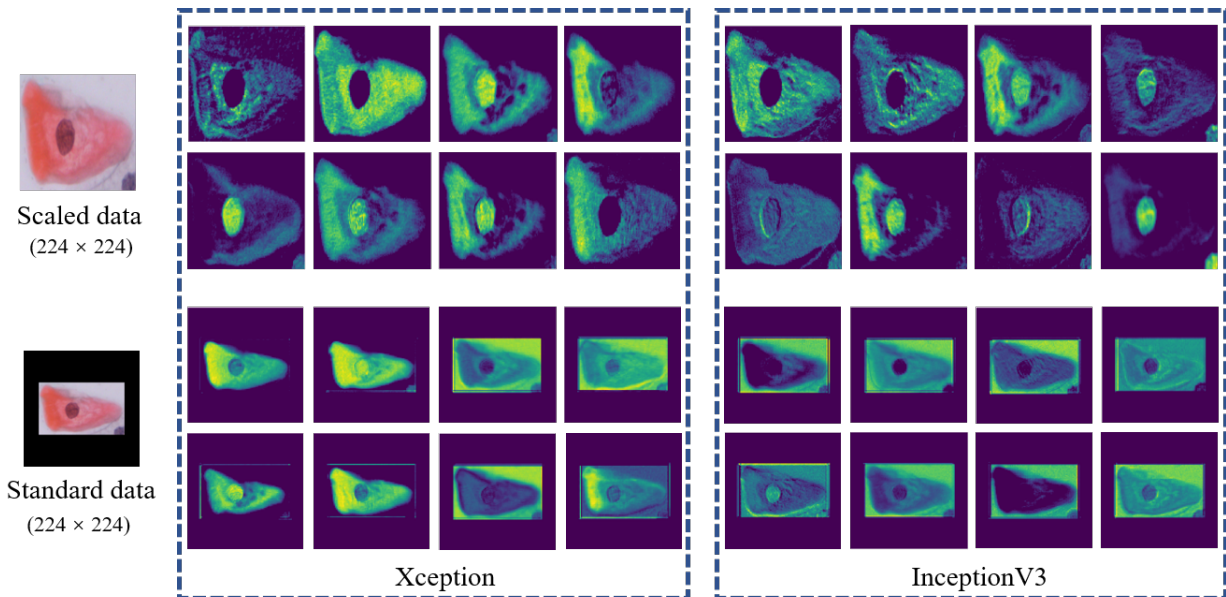


Figure 6: An example of feature maps.

epoch is set to 100, and AdamW optimizer is employed. The batch size of the training set is 32.

4.2. Evaluation method

It is very important to choose an appropriate evaluation method in the comparative experiment. Precision, recall, F1-Score, and accuracy are the most commonly used and most standard evaluation methods in classification experiments [57, 58]. Take the positive-negative binary classification as an example, True Positives (TP) is the number of positive samples accurately predicted. The number of negative samples predicted as positive samples are called False Positives (FP). The number of positive samples predicted as negative samples are called False Negatives (FN). True Negatives (TN) is the number of negative samples accurately predicted. Precision is the proportion of TP among all positive predictions. The recall is the ratio of predicted positive examples to the total number of actual positive examples. F1-Score combines precision and recall. Accuracy is the ratio of the number of correct predictions to the total number of examples. The formulas of the four evaluation methods are shown in Table 3.

4.3. Experimental results and analysis

The average precision, average recall, average F1-Score, and accuracy are used to evaluate models.

Table 3: Evaluation metrics

Assessment	Formula
Precision (P)	$\frac{TP}{TP+FP}$
Recall (R)	$\frac{TP}{TP+FN}$
F1-Score	$2 \times \frac{P \times R}{P+R}$
Accuracy	$\frac{TP+TN}{TP+TN+FP+FN}$

The 5-class classification results are shown in Table 4.

The closed test sets of scaled data and standard data are used to evaluate the generalization ability of models (Table 4). The CNNs that are using the scaled test set, GoogLeNet, reaches the highest test accuracy of 96.03%. The test accuracy of VGG19 is the lowest among all CNNs, with an accuracy of 88.11%. In VTs using the scaled test set, DeiT obtains the highest test accuracy of 95.42%. BoTNet has the lowest accuracy rate of 84.77%. For the CNNs, using the standard data as a test set, the highest classification accuracy of 95.17% is obtained by DenseNet169. The test accuracy of ShuffleNetV2 \times 0.5 is the lowest among the CNNs, with an accuracy of 90.34%. Among all VTs using the standard data as a test set, DeiT has the high-

Table 4: The classification performance of models on the **test set** of SIPaKMeD data.

Models	Scaled data				Standard data			
	Avg. P	Avg. R	Avg. F1	Accuracy	Avg. P	Avg. R	Avg. F1	Accuracy
VGG11	93.70%	93.60%	93.60%	93.56%	93.30%	92.80%	92.90%	92.82%
VGG13	91.60%	91.20%	91.30%	91.21%	93.50%	93.20%	93.30%	93.19%
VGG16	89.80%	89.20%	89.30%	89.23%	92.80%	92.90%	92.80%	92.82%
VGG19	88.60%	88.10%	88.30%	88.11%	91.00%	90.90%	90.90%	90.84%
ResNet18	95.60%	95.50%	95.60%	95.54%	93.80%	93.80%	93.80%	93.81%
ResNet34	94.30%	94.00%	94.10%	94.05%	94.10%	94.00%	94.00%	93.93%
ResNet50	93.10%	92.80%	92.80%	92.82%	94.90%	94.70%	94.70%	94.67%
ResNet101	92.30%	92.00%	92.00%	91.95%	93.70%	93.70%	93.60%	93.68%
DenseNet121	95.80%	95.70%	95.70%	95.66%	95.20%	94.90%	95.00%	94.92%
DenseNet169	95.80%	95.70%	95.70%	95.66%	95.30%	95.20%	95.20%	95.17%
InceptionV3	93.20%	93.00%	93.10%	92.94%	94.00%	93.70%	93.70%	93.68%
Xception	96.10%	95.90%	95.90%	95.91%	95.20%	94.50%	94.60%	94.55%
AlexNet	92.00%	91.90%	91.90%	91.83%	93.50%	93.50%	93.40%	93.44%
GoogLeNet	96.30%	96.00%	96.10%	96.03%	94.30%	94.10%	94.10%	94.05%
MobileNetV2	93.80%	93.70%	93.70%	93.68%	93.10%	93.20%	93.20%	93.19%
ShuffleNetV2×1.0	92.30%	91.90%	91.90%	91.83%	92.80%	92.80%	92.70%	92.69%
ShuffleNetV2×0.5	92.70%	92.30%	92.40%	92.32%	90.40%	90.40%	90.40%	90.34%
InceptionResNetV1	93.80%	93.70%	93.70%	93.68%	94.70%	94.60%	94.60%	94.55%
ViT	93.60%	93.60%	93.60%	93.56%	92.10%	91.90%	91.90%	91.83%
BoTNet	85.80%	84.80%	84.90%	84.77%	91.50%	91.60%	91.50%	91.58%
DeiT	95.50%	95.40%	95.50%	95.42%	94.20%	94.30%	94.20%	94.18%
T2T-ViT	91.90%	91.70%	91.70%	91.70%	88.30%	88.40%	88.30%	88.36%

est test accuracy at 94.18%. The lowest accuracy rate of 88.36%, obtained by T2T-ViT.

Table 5 compares the accuracy of the test dataset using scaled data and standard data. The test accuracy on the standard data is the baseline. In this table, the accuracies of 12 models including VGG11, ResNet18, ResNet34, DenseNet121, DenseNet169, Xception, GoogLeNet, MobileNetV2, ShuffleNetV2×0.5, ViT, DeiT, T2T-ViT tested on scaled data are higher than that of the standard data. The test accuracies of 10 models including VGG13, VGG16, VGG19, ResNet50, ResNet101, InceptionV3, AlexNet, ShuffleNetV2×1.0, InceptionResNetV1, BoTNet are reduced. T2T-ViT increases the most, with an increase of 3.34% and a ratio of 3.78%. BoTNet reduces the most, with a decrease of 6.81%, and a ratio of 7.44%. After calculation, the average change in accuracy is -0.31%. The average of the absolute value of the change in accuracy is 1.76%, and the standard deviation of the absolute value of changes is 1.41%. The average ratio of changes in accuracy is -0.33%. The average of the absolute value of change ratios is 1.90%, and the standard deviation is 1.55%.

It can be seen that the accuracies of some models increase and some decrease. The overall fluctuations are not very large.

It is observed from Table 5 that when the number of layers of the VGG network increases, the classification performance of the scaled data is lower than that of the standard data. And when the number of layers of the ResNet network increases, the classification performance of the scaled data is lower than that of the standard data. In the DenseNet series, the direct connection is introduced between any two layers with the same feature map size, which can be a reason for the better performance on scaled data. The reason for InceptionV3’s poor performance on scaled data should be that one large two-dimensional convolution is replaced with two small one-dimensional convolutions. As an improved version of InceptionV3, the performance of Xception on the scaled data is higher than that on the standard data. AlexNet, which introduces the ReLu activation function, performs worse on scaled data processing. GoogLeNet introduces the inception structure and adopts the Hebbian principle and multi-scale processing, which performs better on scaled data processing. Lightweight networks such

Table 5: Comparison table of scaled data test results and standard data test results in SIPaKMeD dataset. (**Up/down**: The accuracy of the model trained on the scaled data is higher/lower than that of the standard data. **Change**: The change value of the accuracy of the model trained on the scaled data relative to that of the standard data. **Ratio**: The ratio of the change value to the accuracy of the standard data. **Average (abs)** and **Standard deviation (abs)** are calculated from the absolute values of change and ratio of 22 models.)

Models	Up/down	Change	Ratio
VGG11	up	+0.74%	+0.80%
VGG13	down	-1.98%	-2.13%
VGG16	down	-3.59%	-3.87%
VGG19	down	-2.73%	-3.01%
ResNet18	up	+1.73%	+1.84%
ResNet34	up	+0.12%	+0.13%
ResNet50	down	-1.85%	-1.95%
ResNet101	down	-1.73%	-1.85%
DenseNet121	up	+0.74%	+0.78%
DenseNet169	up	+0.49%	+0.52%
InceptionV3	down	-0.74%	-0.79%
Xception	up	+1.36%	+1.44%
AlexNet	down	-1.61%	-1.72%
GoogLeNet	up	+1.98%	+2.11%
MobileNetV2	up	+0.49%	+0.53%
ShuffleNetV2×1.0	down	-0.86%	-0.93%
ShuffleNetV2×0.5	up	+1.98%	+2.19%
InceptionResNetV1	down	-0.87%	-0.92%
ViT	up	+1.73%	+1.88%
BoTNet	down	- 6.81%	- 7.44%
DeiT	up	+1.24%	+1.31%
T2T-ViT	up	+ 3.34%	+ 3.78%
Average	down	-0.31%	-0.33%
Average (abs)	-	1.76%	1.90%
Standard deviation (abs)	-	1.41%	1.55%

as MobileNet and ShuffleNet have more advantages in processing scaled data.

In VTs, models basically have a better effect on the scaled data than the standard data. It is because the Transformer pays more attention to global information and lacks local perception.

In the case of classifying the scaled data with missing internal cell ratio information, the classification effects of some models are slightly lower than that of the standard data, but the declines are not large. Even, the effects of some models have been improved. So it shows that the deep learning method is very robust to changes in the internal cell ratio of cervical cytopathological images.

In order to further investigate whether the results are stable, the following extended experiments are carried out.

4.4. Extended experiment

4.4.1. Extended experiment on SIPaKMeD dataset: Five-fold cross-validation

The classification performance of models of the five-fold cross-validation experiment on the SIPaKMeD dataset is shown in Table 7. In this table, among all CNNs trained on scaled data, Xception has the highest classification accuracy, 87.95%. Among all VTs trained on scaled data, DeiT has the highest accuracy of 85.16%. With CNNs trained on standard data, the accuracy of Xception is still the highest, 88.83%. Among all VTs trained on standard data, T2T-ViT obtains the highest accuracy.

Table 6: Comparison table of scaled data validation results and standard data validation results of the five-fold cross-validation experiment on the SIPaKMeD dataset. (**Up/down**: The accuracy of the model trained on the scaled data is higher/lower than that of the standard data. **Change**: The change value of the accuracy of the model trained on the scaled data relative to that of the standard data. **Ratio**: The ratio of the change value to the accuracy of the standard data. **Average (abs)** and **Standard deviation (abs)** are calculated from the absolute values of change and ratio of 22 models.)

Models	Up/down	Change	Ratio
VGG11	down	-1.90%	-2.25%
VGG13	down	-1.61%	-1.86%
VGG16	down	-3.13%	-3.80%
VGG19	down	-4.61%	-5.43%
ResNet18	down	-1.09%	-1.24%
ResNet34	down	-0.56%	-0.65%
ResNet50	down	- 5.00%	- 5.73%
ResNet101	down	-4.41%	-5.11%
DenseNet121	down	-3.23%	-3.73%
DenseNet169	down	-1.01%	-1.17%
InceptionV3	down	-2.50%	-2.90%
Xception	down	-0.88%	-0.99%
AlexNet	down	-4.03%	-4.73%
GoogLeNet	down	-2.32%	-2.65%
MobileNetV2	down	-0.39%	-0.46%
ShuffleNetV2×1.0	up	+0.03%	+0.03%
ShuffleNetV2×0.5	down	-0.57%	-0.68%
InceptionResNetV1	down	-1.93%	-2.21%
ViT	up	+ 2.07%	+ 2.55%
BoTNet	down	-3.43%	-4.21%
DeiT	up	+0.07%	+0.08%
T2T-ViT	down	-1.55%	-1.82%
Average	down	-1.91%	-2.23%
Average (abs)	-	2.11%	2.47%
Standard deviation (abs)	-	1.48%	1.74%

The comparison of the validation results between the scaled data and standard data of the five-fold cross-validation experiment on the SIPaKMeD dataset is shown in Table 6. In

Table 7: The classification performance of models of the **five-fold cross-validation** experiment on the SIPaKMeD dataset.

Models	Scaled data				Standard data			
	Avg. P	Avg. R	Avg. F1	Accuracy	Avg. P	Avg. R	Avg. F1	Accuracy
VGG11	84.58%	82.88%	82.42%	82.79%	86.04%	84.74%	84.40%	84.69%
VGG13	85.56%	84.84%	84.76%	84.79%	87.40%	86.42%	86.10%	86.40%
VGG16	82.20%	79.26%	78.52%	79.27%	84.18%	82.44%	81.78%	82.40%
VGG19	82.10%	80.38%	80.18%	80.37%	85.90%	85.04%	85.14%	84.99%
ResNet18	87.68%	86.46%	85.94%	86.42%	88.10%	87.62%	87.26%	87.50%
ResNet34	87.16%	86.28%	85.72%	86.23%	87.76%	86.86%	86.62%	86.79%
ResNet50	84.18%	82.22%	81.56%	82.25%	88.00%	87.30%	87.24%	87.26%
ResNet101	83.74%	82.04%	81.60%	81.98%	86.56%	86.50%	86.30%	86.39%
DenseNet121	85.06%	83.60%	82.78%	83.58%	87.50%	86.86%	86.62%	86.81%
DenseNet169	86.76%	85.72%	85.36%	85.65%	88.28%	86.70%	86.06%	86.67%
InceptionV3	85.44%	83.66%	83.46%	83.65%	87.12%	86.18%	85.98%	86.15%
Xception	89.06%	87.98%	87.84%	87.95%	89.76%	88.94%	88.76%	88.83%
AlexNet	83.20%	81.14%	80.84%	81.09%	86.26%	85.16%	84.76%	85.11%
GoogLeNet	87.18%	85.22%	84.82%	85.18%	88.94%	87.58%	87.46%	87.51%
MobileNetV2	86.76%	84.96%	84.76%	84.94%	86.50%	85.38%	85.18%	85.33%
ShuffleNetV2×1.0	85.92%	84.54%	83.82%	84.52%	85.92%	84.56%	84.00%	84.49%
ShuffleNetV2×0.5	83.54%	82.58%	82.26%	82.52%	84.58%	83.16%	82.66%	83.08%
InceptionResNetV1	87.02%	85.20%	84.96%	85.23%	88.00%	87.22%	87.04%	87.16%
ViT	85.72%	83.36%	82.70%	83.33%	82.18%	81.30%	80.10%	81.26%
BoTNet	79.60%	78.06%	76.44%	78.05%	82.50%	81.56%	81.12%	81.48%
DeiT	86.32%	85.16%	84.74%	85.16%	86.68%	85.14%	84.66%	85.09%
T2T-ViT	85.64%	83.58%	83.28%	83.61%	85.80%	85.24%	84.98%	85.16%

this table, the accuracies of three models including ShuffleNetV2×1.0, ViT, DeiT trained on scaled data are higher than that of standard data. The accuracies of 19 models including VGG11, VGG13, VGG16, VGG19, ResNet18, ResNet34, ResNet50, ResNet101, DenseNet121, DenseNet169, InceptionV3, Xception, AlexNet, GoogLeNet, MobileNetV2, ShuffleNetV2×0.5, InceptionResNetV1, BoTNet, T2T-ViT trained on scaled data are lower than that of standard data. The model with the most increase in accuracy is ViT, with 2.07% and the increase rate is 2.55%. ResNet50’s accuracy reduces the most, with 5.00% and the ratio is 5.73%. After calculation, the average change in accuracy is -1.91%. The average of the absolute value of the change in accuracy is 2.11%, and the standard deviation of the absolute value of changes is 1.48%. The average ratio of changes in accuracy is -2.23%. The average of the absolute value of change ratios is 2.47%, and the standard deviation is 1.74%.

The overall situation is still that the accuracies of some models increase, and some decrease. And the fluctuations are not very large. As can be seen in Table 6, after using the five-fold cross-validation method, compared with Table 5, the performance

of the ResNet, DenseNet, Xception, GoogLeNet on the scaled data are lower than that on the standard data. The rest is basically the same. It still shows that the deep learning method is very robust to the changes in the internal cell ratio of cervical cytopathological images.

4.4.2. Extended experiment on SIPaKMeD dataset: classification with data augmentation

The classification performance on the test set of SIPaKMeD augmented data is shown in Table 8. In this table, In CNNs trained on scaled data, ResNet18 has the highest accuracy, which is 97.15%. In VTs trained on scaled data, ViT has the highest accuracy rate of 95.54%. In CNNs trained on standard data, GoogLeNet is the model with the highest accuracy, 97.40%. In VTs trained on standard data, DeiT has the highest accuracy rate.

Table 9 compares the accuracy of the test dataset using scaled data and standard data. The accuracies of eight models including VGG11, ResNet18, ResNet34, ResNet101, Xception, ShuffleNetV2×1.0, ViT, T2T-ViT trained on scaled data are higher than that of standard data. The accuracies of 13 models including VGG13, VGG16,

Table 8: The classification performance of models on the **test set** of SIPaKMeD augmented data.

Models	Scaled data				Standard data			
	Avg. P	Avg. R	Avg. F1	Accuracy	Avg. P	Avg. R	Avg. F1	Accuracy
VGG11	96.20%	96.20%	96.10%	96.03%	95.20%	94.80%	94.90%	94.80%
VGG13	94.70%	94.60%	94.60%	94.55%	96.30%	96.30%	96.30%	96.28%
VGG16	94.10%	93.90%	94.00%	93.93%	95.30%	95.10%	95.20%	95.17%
VGG19	93.10%	92.50%	92.70%	92.57%	95.30%	95.20%	95.20%	95.17%
ResNet18	97.20%	97.20%	97.20%	97.15%	96.90%	96.80%	96.80%	96.78%
ResNet34	96.30%	96.20%	96.20%	96.16%	96.10%	96.00%	96.10%	96.03%
ResNet50	95.60%	95.60%	95.60%	95.54%	96.20%	96.20%	96.10%	96.03%
ResNet101	96.00%	95.90%	95.90%	95.91%	95.80%	95.70%	95.70%	95.66%
DenseNet121	96.90%	96.90%	96.90%	96.90%	97.10%	97.10%	97.00%	97.02%
DenseNet169	96.30%	96.20%	92.00%	96.16%	96.60%	96.50%	96.50%	96.53%
InceptionV3	95.40%	95.20%	95.20%	95.17%	96.80%	96.80%	96.80%	96.78%
Xception	97.00%	97.10%	97.00%	97.02%	96.10%	96.10%	95.80%	95.79%
AlexNet	95.10%	94.90%	94.90%	94.92%	95.60%	95.70%	95.70%	95.66%
GoogLeNet	96.80%	96.80%	96.80%	96.78%	97.50%	97.40%	97.40%	97.40%
MobileNetV2	96.50%	96.60%	96.50%	96.53%	96.80%	96.80%	96.80%	96.78%
ShuffleNetV2×1.0	96.90%	96.80%	96.80%	96.78%	96.10%	96.10%	96.10%	96.03%
ShuffleNetV2×0.5	95.30%	95.20%	95.20%	95.17%	95.90%	95.80%	95.80%	95.79%
InceptionResNetV1	95.10%	95.10%	95.00%	95.04%	97.20%	97.20%	97.20%	97.15%
ViT	95.80%	95.60%	95.60%	95.54%	93.10%	93.00%	93.00%	92.94%
BoTNet	87.60%	87.60%	87.50%	87.62%	88.90%	89.00%	88.90%	88.98%
DeiT	95.10%	95.00%	95.00%	94.92%	95.00%	94.90%	95.00%	94.92%
T2T-ViT	94.50%	94.50%	94.40%	94.43%	92.20%	92.10%	92.10%	92.07%

VGG19, ResNet50, DenseNet121, DenseNet169, InceptionV3, AlexNet, GoogLeNet, MobileNetV2, ShuffleNetV2×0.5, InceptionResNetV1, BoTNet are reduced and the accuracy of DeiT is equal. The most improved model is ViT, which has an increase of 2.60% and the increase rate is 2.80%. The accuracy of VGG19 reduces the most, with 2.60% and the ratio is 2.73%. After calculation, the average change in accuracy is -0.22%. The average of the absolute value of the change in accuracy is 1.04%, and the standard deviation of the absolute value of changes is 0.81%. The average ratio of changes in accuracy is -0.23%. The average of the absolute value of change ratios is 1.09%, and the standard deviation is 0.86%.

Overall, the accuracies of some models increase, and some decrease. It can be seen from Table 9 that after data augmentation, compared with Table 5, the performance of the DenseNet and Lightweight networks on the scaled data are lower than on the standard data. The rest is basically the same. Therefore, after augmenting the training data, some redundant information appears, resulting in a negative impact on some models. It still shows that the deep learning method is very robust

to the changes in the internal cell ratio of cervical cytopathological images.

4.4.3. Extended experiment on Herlev dataset

The two-class classification performance on the test set of Herlev augmented data is shown in Table 11. In this table, in CNNs trained on scaled data, GoogLeNet has the highest classification accuracy, 93.44%. Among all VTs trained on scaled data, DeiT has the highest accuracy of 93.44%. With the CNNs trained on standard data, DenseNet121 is the model with the highest accuracy, 95.08%. In VTs trained on standard data, T2T-ViT obtains the highest accuracy.

Table 10 compares the accuracy of the test dataset using scaled data and standard data. The accuracies of 14 models including VGG11, ResNet34, ResNet101, DenseNet169, Xception, AlexNet, GoogLeNet, MobileNetV2, ShuffleNetV2×1.0, ShuffleNetV2×0.5, Inception-ResNetV1, ViT, BoTNet, DeiT trained on scaled data are higher than that of the standard data and the accuracies of eight models including VGG13, VGG16, VGG19, ResNet18, ResNet50, DenseNet121, InceptionV3, T2T-ViT are reduced.

Table 9: Comparison table of test results between the augmented scaled data and standard data in SIPaKMeD dataset. (**Up/down**: The accuracy of the model trained on the scaled data is higher/lower than that of the standard data. **Change**: The change value of the accuracy of the model trained on the scaled data relative to that of the standard data. **Ratio**: The ratio of the change value to the accuracy of the standard data. **Average (abs)** and **Standard deviation (abs)** are calculated from the absolute values of change and ratio of 22 models.)

Models	Up/down	Change	Ratio
VGG11	up	+1.23%	+1.30%
VGG13	down	-1.73%	-1.80%
VGG16	down	-1.24%	-1.30%
VGG19	down	-2.60%	-2.73%
ResNet18	up	+0.37%	+0.38%
ResNet34	up	+0.13%	+0.14%
ResNet50	down	-0.49%	-0.51%
ResNet101	up	+0.25%	+0.26%
DenseNet121	down	-0.12%	-0.12%
DenseNet169	down	-0.37%	-0.38%
InceptionV3	down	-1.61%	-1.66%
Xception	up	+1.23%	+1.28%
AlexNet	down	-0.74%	-0.77%
GoogLeNet	down	-0.62%	-0.64%
MobileNetV2	down	-0.25%	-0.26%
ShuffleNetV2×1.0	up	+0.75%	+0.78%
ShuffleNetV2×0.5	down	-0.62%	-0.65%
InceptionResNetV1	down	-2.11%	-2.17%
ViT	up	+2.60%	+2.80%
BoTNet	down	-1.36%	-1.53%
DeiT	equal	0.00%	0.00%
T2T-ViT	up	+2.36%	+2.56%
Average	down	-0.22%	-0.23%
Average (abs)	-	1.04%	1.09%
Standard deviation (abs)	-	0.81%	0.86%

The model with the largest improvement is ViT, which has the increase of 7.10% and the ratio of 8.33%. The accuracy of VGG19 reduces the most, down 14.75%, with the ratio of 16.66%. After calculation, the average change in accuracy is +0.27%. The average of the absolute value of the change in accuracy is 2.71%, and the standard deviation of the absolute value of changes is 3.11%. The average ratio of changes in accuracy is +0.33%. The average of the absolute value of change ratios is 3.05%, and the standard deviation is 3.55%.

The overall trends are still that the accuracies of some models increase, and some decrease. Since the small amount of data in the Herlev dataset and the high class imbalance of the two categories, the classification performance is reduced compared with the SIPaKMeD experiment. But overall, the accuracies of models do not fluctuate too much. On

Table 10: Comparison table of test results between the augmented scaled data and standard data in Herlev dataset. (**Up/down**: The accuracy of the model trained on the scaled data is higher/lower than that of the standard data. **Change**: The change value of the accuracy of the model trained on the scaled data relative to that of the standard data. **Ratio**: The ratio of the change value to the accuracy of the standard data. **Average (abs)** and **Standard deviation (abs)** are calculated from the absolute values of change and ratio of 22 models.)

Models	Up/down	Change	Ratio
VGG11	up	+0.54%	+0.62%
VGG13	down	-2.73%	-2.97%
VGG16	down	-1.64%	-1.84%
VGG19	down	-14.75%	-16.66%
ResNet18	down	-0.55%	-0.59%
ResNet34	up	+1.09%	+1.21%
ResNet50	down	-1.09%	-1.18%
ResNet101	up	+0.54%	+0.59%
DenseNet121	down	-2.74%	-2.88%
DenseNet169	up	+1.09%	+1.19%
InceptionV3	down	-1.10%	-1.21%
Xception	up	+1.64%	+1.80%
AlexNet	up	+2.73%	+3.08%
GoogLeNet	up	+3.28%	+3.64%
MobileNetV2	up	+1.64%	+1.84%
ShuffleNetV2×1.0	up	+1.09%	+1.21%
ShuffleNetV2×0.5	up	+3.82%	+4.32%
InceptionResNetV1	up	+0.54%	+0.60%
ViT	up	+7.10%	+8.33%
BoTNet	up	+1.64%	+1.86%
DeiT	up	+6.01%	+6.87%
T2T-ViT	down	-2.26%	-2.51%
Average	up	+0.27%	+0.33%
Average (abs)	-	2.71%	3.05%
Standard deviation (abs)	-	3.11%	3.55%

the Herlev dataset, it is still consistent with the conclusion that the deep learning method is very robust to the changes in the internal cell ratio of cervical cytopathological images.

5. Conclusion and future work

The image input required by the deep learning model is usually consistent, but the size of many clinical medical images are inconsistent. The internal cell ratios of the images are suffered while resizing it directly. Clinically, the ratios of cells inside cytopathological images provide important information for doctors to diagnose cancer. Therefore, it is illogical to resize directly. However, many existing studies directly resize images, and the results are still robust. In order to find a reasonable explanation, cervical cells are used as an example

Table 11: The two-class classification performance of models on the **test set** of Herlev augmented data.

Models	Scaled data				Standard data			
	Avg. P	Avg. R	Avg. F1	Accuracy	Avg. P	Avg. R	Avg. F1	Accuracy
VGG11	86.00%	81.80%	83.60%	87.97%	85.50%	80.80%	82.70%	87.43%
VGG13	89.90%	81.20%	84.30%	89.07%	90.70%	87.70%	89.00%	91.80%
VGG16	86.10%	80.10%	82.40%	87.43%	86.60%	84.50%	85.50%	89.07%
VGG19	36.90%	50.00%	42.40%	73.77%	90.50%	79.40%	83.00%	88.52%
ResNet18	93.20%	86.80%	89.40%	92.34%	91.50%	89.80%	90.60%	92.89%
ResNet34	92.40%	84.70%	87.60%	91.25%	88.10%	86.00%	86.90%	90.16%
ResNet50	89.10%	88.00%	88.60%	91.25%	93.20%	86.80%	89.40%	92.34%
ResNet101	91.00%	88.70%	89.80%	92.34%	88.70%	91.10%	89.80%	91.80%
DenseNet121	91.70%	88.10%	89.70%	92.34%	96.00%	91.30%	93.40%	95.08%
DenseNet169	91.50%	89.80%	90.60%	92.89%	89.60%	89.10%	89.30%	91.80%
InceptionV3	87.50%	84.90%	86.10%	89.61%	89.70%	85.60%	87.40%	90.71%
Xception	92.80%	88.50%	90.40%	92.89%	89.10%	88.00%	88.60%	91.25%
AlexNet	91.60%	85.30%	87.80%	91.25%	86.50%	82.80%	84.40%	88.52%
GoogLeNet	91.10%	92.20%	91.60%	93.44%	90.70%	83.30%	86.10%	90.16%
MobileNetV2	90.40%	85.00%	87.10%	90.71%	89.00%	81.90%	84.60%	89.07%
ShuffleNetV2×1.0	92.40%	84.70%	87.60%	91.25%	90.70%	83.30%	86.10%	90.16%
ShuffleNetV2×0.5	90.60%	89.40%	90.00%	92.34%	90.50%	79.40%	83.00%	88.52%
InceptionResNetV1	90.80%	86.00%	88.00%	91.25%	88.60%	87.00%	87.80%	90.71%
ViT	89.70%	90.80%	90.20%	92.34%	86.80%	73.90%	77.40%	85.24%
BoTNet	91.30%	81.60%	84.90%	89.61%	90.10%	78.40%	82.00%	87.97%
DeiT	91.50%	91.50%	91.60%	93.44%	88.50%	78.00%	81.40%	87.43%
T2T-ViT	84.70%	83.80%	84.20%	87.90%	91.70%	82.60%	85.90%	90.16%

to test the robustness of the deep learning method. First of all, the raw data are standardized and resized directly to get the standard and scaled data, respectively. Then the standard and scaled data are resized to 224×224 pixels. Finally, twenty-two deep learning models are used to classify standard data and scaled data. Through the experimental results, it can be observed that in the case of classifying the scaled data without internal cell ratio information, the classification effects of some models are slightly lower than that of the standard data, but the declines are not large. Even, the effects of some models have been improved. The final conclusion is that the deep learning method is robust to changes in the internal cell ratio of cervical cytopathological images.

The limitation of this study is that the input images must be cytopathological images that contain cell ratios.

Recently, the popular Transformer surpasses the CNN network in the field of computer vision. In this study, Transformer does not show amazing results, and BoTNet combined with Transformer and ResNet does not perform well on cervical cell images, either. We assume that combining Xception,

which performs well in this study, with Transformer may result in better performance. Transformer focus on global information, so we can fuse Transformer and classical local features to obtain better classification performance. In the future, we can also try to use more new VTs to classify medical images and make improvements and supplements based on the structure of the model. In addition, standardization and centralization can be used as data preprocessing, which may increase the accuracy of the model.

References

- [1] G. Bugdayci, M. B. Pehlivan, M. Basol, O. M. Yis, Roles of the systemic inflammatory response biomarkers in the diagnosis of cancer patients with solid tumors, *Experimental Biomedical Research* 2 (1) (2019) 37–43. doi:<https://doi.org/10.30714/j-ebr.2019147582>.
- [2] J. Ferlay, M. Ervik, F. Lam, M. Colombet, L. Mery, M. Piñeros, A. Znaor, I. Soerjomataram, F. Bray, Global cancer observatory: cancer today, Lyon, France: International Agency for Research on Cancer. URL <https://gco.iarc.fr/today/>
- [3] Chaturvedi, K. Anil, Epidemiology and clinical aspects of hpv in head and neck cancers, *Head Neck Pathol* 6 (1 Supplement) (2012) 16–24. doi:<https://doi.org/10.1007/s12105-012-0377-0>.

- [4] H. U. Bernard, R. D. Burk, Z. Chen, K. V. Doorslaer, H. Z. Hausen, E. Villiers, Classification of papillomaviruses (pvs) based on 189 pv types and proposal of taxonomic amendments., *Virology* 401 (1) (2010) 70–79. doi:<https://doi.org/10.1016/j.virol.2010.02.002>.
- [5] E. J. Crosbie, M. H. Einstein, S. Franceschi, H. C. Kitchener, Human papillomavirus and cervical cancer, *The Lancet* 382 (9895) (2013) 889–899. doi:[https://doi.org/10.1016/S0140-6736\(07\)61416-0](https://doi.org/10.1016/S0140-6736(07)61416-0).
- [6] W. F. Cheng, Human papillomavirus vaccine for cervical cancer: Where are we now?, *Taiwanese Journal of Obstetrics Gynecology* 44 (3) (2005) 391–391. doi:[https://doi.org/10.1016/S1028-4559\(09\)60145-5](https://doi.org/10.1016/S1028-4559(09)60145-5).
- [7] S. S. De, M. Diaz, X. Castellsague, G. Clifford, L. Bruni, Worldwide prevalence and genotype distribution of cervical human papillomavirus dna in women with normal cytology: a meta-analysis., *Lancet Infect. Dis.* 7 (7) (2007) 453–459. doi:[https://doi.org/10.1016/S1473-3099\(07\)70158-5](https://doi.org/10.1016/S1473-3099(07)70158-5).
- [8] F. X. Bosch, A. N. Burchell, M. Schiffman, A. R. Giuliano, S. de Sanjose, L. Bruni, G. Tortolero-Luna, S. K. Kjaer, N. Muñoz, Epidemiology and natural history of human papillomavirus infections and type-specific implications in cervical neoplasia, *Vaccine* 26 (2008) K1–K16. doi:<https://doi.org/10.1016/j.vaccine.2008.05.064>.
- [9] T. Šarenac, M. Mikov, Cervical cancer, different treatments and importance of bile acids as therapeutic agents in this disease, *Front. Pharmacol.* 10 (2019) 484. doi:<https://doi.org/10.3389/fphar.2019.00484>.
- [10] D. Saslow, D. Solomon, H. W. Lawson, M. Killackey, S. L. Kulasingam, J. Cain, F. A. Garcia, A. T. Moriarty, A. G. Waxman, D. C. Wilbur, et al., American cancer society, american society for colposcopy and cervical pathology, and american society for clinical pathology screening guidelines for the prevention and early detection of cervical cancer, *CA: a cancer journal for clinicians* 62 (3) (2012) 147–172. doi:<https://doi.org/10.3322/caac.21139>.
- [11] E. Davey, A. Barratt, L. Irwig, S. F. Chan, A. M. Saville, Effect of study design and quality on unsatisfactory rates, cytology classifications, and accuracy in liquid-based versus conventional cervical cytology: a systematic review., *The Lancet* 367 (9505) (2006) 122–132. doi:[https://doi.org/10.1016/S0140-6736\(06\)67961-0](https://doi.org/10.1016/S0140-6736(06)67961-0).
- [12] A. Gençtav, S. Aksoy, S. Önder, Unsupervised segmentation and classification of cervical cell images, *Pattern Recognit.* 45 (12) (2012) 4151–4168. doi:<https://doi.org/10.1016/j.patcog.2012.05.006>.
- [13] M. M. Rahaman, C. Li, X. Wu, Y. Yao, S. Qi, A survey for cervical cytopathology image analysis using deep learning, *IEEE Access* PP (99) (2020) 1–1. doi:<https://doi.org/10.1109/ACCESS.2020.2983186>.
- [14] Y. LeCun, Y. Bengio, G. Hinton, Deep learning, *nature* 521 (7553) (2015) 436–444. doi:<https://doi.org/10.1038/nature14539>.
- [15] F. Xing, L. Yang, Robust nucleus/cell detection and segmentation in digital pathology and microscopy images: A comprehensive review, *IEEE Rev Biomed Eng* (2016) 234–263doi:<https://doi.org/10.1109/RBME.2016.2515127>.
- [16] I. Goodfellow, Y. Bengio, A. Courville, Y. Bengio, *Deep learning*, MIT press, 2016. doi:<https://doi.org/10.4258/hir.2016.22.4.351>.
- [17] M. S. Landau, L. Pantanowitz, Artificial intelligence in cytopathology: a review of the literature and overview of commercial landscape, *Journal of the American Society of Cytopathology* 8 (4) (2019) 230–241. doi:<https://doi.org/10.1016/j.jasc.2019.03.003>.
- [18] G. Hinton, Deep learning—a technology with the potential to transform health care, *Jama* 320 (11) (2018) 1101–1102. doi:<https://doi.org/10.1001/jama.2018.11100>.
- [19] Y. Lecun, K. Kavukcuoglu, C. Farabet, Convolutional networks and applications in vision, in: *Proceedings of 2010 IEEE International Symposium on Circuits and Systems*, 2010. doi:<https://doi.org/10.1109/ISCAS.2010.5537907>.
- [20] A. Dosovitskiy, L. Beyer, A. Kolesnikov, D. Weissenborn, X. Zhai, T. Unterthiner, M. Dehghani, M. Minderer, G. Heigold, S. Gelly, et al., An image is worth 16x16 words: Transformers for image recognition at scale, *arXiv preprint arXiv:2010.11929*. URL <https://arxiv.org/abs/2010.11929>
- [21] C. Zhao, X. Zhou, L. Sui, M. Yang, *Cervical Cancer Screening and Clinical Management: Cytology, Histology, Colposcopy*, Beijing Science and Technology Press, 2017.
- [22] M. E. Plissiti, P. Dimitrakopoulos, G. Sfikas, C. Nikou, O. Krikoni, A. Charchanti, Sipakmed: A new dataset for feature and image based classification of normal and pathological cervical cells in pap smear images, in: *2018 25th IEEE International Conference on Image Processing (ICIP)*, IEEE, 2018, pp. 3144–3148. doi:<https://doi.org/10.1109/ICIP.2018.8451588>.
- [23] K. Simonyan, A. Zisserman, Very deep convolutional networks for large-scale image recognition, *arXiv preprint arXiv:1409.1556*. URL <https://arxiv.org/abs/1409.1556>
- [24] K. He, X. Zhang, S. Ren, J. Sun, Deep residual learning for image recognition, in: *Proceedings of the IEEE conference on computer vision and pattern recognition*, 2016, pp. 770–778. doi:<https://doi.org/10.1109/CVPR.2016.90>.
- [25] G. Huang, Z. Liu, L. Van Der Maaten, K. Q. Weinberger, Densely connected convolutional networks, in: *Proceedings of the IEEE conference on computer vision and pattern recognition*, 2017, pp. 4700–4708. doi:<https://doi.org/10.1109/CVPR.2017.243>.
- [26] C. Szegedy, V. Vanhoucke, S. Ioffe, J. Shlens, Z. Wojna, Rethinking the inception architecture for computer vision, in: *Proceedings of the IEEE conference on computer vision and pattern recognition*, 2016, pp. 2818–2826. doi:<https://doi.org/10.1109/CVPR.2016.308>.
- [27] F. Chollet, Xception: Deep learning with depthwise separable convolutions, in: *2017 IEEE Conference on Computer Vision and Pattern Recognition (CVPR)*, 2017, pp. 1800–1807. doi:<https://doi.org/10.1109/CVPR.2017.195>.
- [28] O. Russakovsky, J. Deng, H. Su, J. Krause, S. Satheesh, S. Ma, Z. Huang, A. Karpathy, A. Khosla, M. Bernstein, et al., Imagenet large scale visual recognition challenge, *Int. J. Comput. Vision* 115 (3) (2015) 211–252. doi:<https://doi.org/10.1007/s11263-015-0816-y>.
- [29] C. Szegedy, W. Liu, Y. Jia, P. Sermanet, S. Reed, D. Anguelov, D. Erhan, V. Vanhoucke, A. Rabinovich, Going deeper with convolutions, in: *2015 IEEE Conference on Computer Vision and Pattern Recognition (CVPR)*, 2015, pp. 1–9. doi:<https://doi.org/10.1109/CVPR.2015.7171971>.

- 1109/CVPR.2015.7298594.
- [30] M. Sandler, A. Howard, M. Zhu, A. Zhmoginov, L.-C. Chen, Mobilenetv2: Inverted residuals and linear bottlenecks, in: Proceedings of the IEEE conference on computer vision and pattern recognition, 2018, pp. 4510–4520. doi:<https://doi.org/10.1109/CVPR.2018.00474>.
- [31] N. Ma, X. Zhang, H.-T. Zheng, J. Sun, Shufflenet v2: Practical guidelines for efficient cnn architecture design, in: Proceedings of the European conference on computer vision (ECCV), 2018, pp. 116–131. doi:https://doi.org/10.1007/978-3-030-01264-9_8.
- [32] C. Szegedy, S. Ioffe, V. Vanhoucke, A. A. Alemi, Inception-v4, inception-resnet and the impact of residual connections on learning, in: Proceedings of the Thirty-First AAAI Conference on Artificial Intelligence, 2017, p. 4278–4284. URL <https://dl.acm.org/doi/10.5555/3298023.3298188>
- [33] A. Srinivas, T.-Y. Lin, N. Parmar, J. Shlens, P. Abbeel, A. Vaswani, Bottleneck transformers for visual recognition, arXiv preprint arXiv:2101.11605. URL <https://arxiv.org/abs/2101.11605>
- [34] H. Touvron, M. Cord, M. Douze, F. Massa, A. Sablayrolles, H. Jegou, Training data-efficient image transformers & distillation through attention, in: Proceedings of the 38th International Conference on Machine Learning, Vol. 139, 2021, p. 1. URL <https://proceedings.mlr.press/v139/touvron21a>
- [35] L. Yuan, Y. Chen, T. Wang, W. Yu, Y. Shi, F. E. Tay, J. Feng, S. Yan, Tokens-to-token vit: Training vision transformers from scratch on imagenet, arXiv preprint arXiv:2101.11986. URL <https://arxiv.org/abs/2101.11986>
- [36] L. Zhang, L. Lu, I. Nogues, R. M. Summers, S. Liu, J. Yao, Deeppap: deep convolutional networks for cervical cell classification, IEEE J. Biomed. Health. Inf. 21 (6) (2017) 1633–1643. doi:<https://doi.org/10.1109/JBHI.2017.2705583>.
- [37] J. Hyeon, H.-J. Choi, K. N. Lee, B. D. Lee, Automating papanicolaou test using deep convolutional activation feature, in: 2017 18th IEEE International Conference on Mobile Data Management (MDM), IEEE, 2017, pp. 382–385. doi:<https://doi.org/10.1109/MDM.2017.66>.
- [38] B. Taha, J. Dias, N. Werghi, Classification of cervical-cancer using pap-smear images: a convolutional neural network approach, in: Annual Conference on Medical Image Understanding and Analysis, Springer, 2017, pp. 261–272. doi:https://doi.org/10.1007/978-3-319-60964-5_23.
- [39] H. Wieslander, G. Forslid, E. Bengtsson, C. Wahlby, J.-M. Hirsch, C. Runow Stark, S. Kecheril Sadanandan, Deep convolutional neural networks for detecting cellular changes due to malignancy, in: Proceedings of the IEEE International Conference on Computer Vision Workshops, 2017, pp. 82–89. doi:<https://doi.org/10.1109/ICCVW.2017.18>.
- [40] S. Gautam, N. Jith, A. K. Sao, A. Bhavsar, A. Natarajan, et al., Considerations for a pap smear image analysis system with cnn features, arXiv preprint arXiv:1806.09025. URL <https://arxiv.org/abs/1806.09025>
- [41] Y. Promworn, S. Pattanasak, C. Pintavirooj, W. Piyawattanametha, Comparisons of pap smear classification with deep learning models, in: 2019 IEEE 14th International Conference on Nano/Micro Engineered and Molecular Systems (NEMS), IEEE, 2019, pp. 282–285. doi:<https://doi.org/10.1109/NEMS.2019.8915600>.
- [42] L. D. Nguyen, R. Gao, D. Lin, Z. Lin, Biomedical image classification based on a feature concatenation and ensemble of deep cnns, J. Ambient Intell. Hum. Comput. (2019) 1–13doi:<https://doi.org/10.1007/s12652-019-01276-4>.
- [43] Kurnianingsih, K. Allehaibi, L. E. Nugroho, Widyawan, T. Mantoro, Segmentation and classification of cervical cells using deep learning, IEEE Access PP (99) (2019) 1–1. doi:<https://doi.org/10.1109/ACCESS.2019.2936017>.
- [44] K. K. GV, G. M. Reddy, Automatic classification of whole slide pap smear images using cnn with pca based feature interpretation., in: CVPR Workshops, 2019, pp. 1074–1079. doi:<https://doi.org/10.1109/CVPRW.2019.00140>.
- [45] D. Xue, X. Zhou, C. Li, Y. Yao, M. M. Rahaman, J. Zhang, H. Chen, J. Zhang, S. Qi, H. Sun, An application of transfer learning and ensemble learning techniques for cervical histopathology image classification, IEEE Access 8 (2020) 104603–104618. doi:<https://doi.org/10.1109/ACCESS.2020.2999816>.
- [46] N. Dong, L. Zhao, C.-H. Wu, J.-F. Chang, Inception v3 based cervical cell classification combined with artificially extracted features, Appl. Soft Comput. 93 (2020) 106311. doi:<https://doi.org/10.1016/j.asoc.2020.106311>.
- [47] K. P. Win, Y. Kitjaidure, K. Hamamoto, T. Myo Aung, Computer-assisted screening for cervical cancer using digital image processing of pap smear images, Applied Sciences 10 (5) (2020) 1800. doi:<https://doi.org/10.3390/app10051800>.
- [48] A. Khamparia, D. Gupta, V. H. C. de Albuquerque, A. K. Sangaiah, R. H. Jhaveri, Internet of health things-driven deep learning system for detection and classification of cervical cells using transfer learning, The Journal of Supercomputing (2020) 1–19doi:<https://doi.org/10.1007/s11227-020-03159-4>.
- [49] A. Khamparia, D. Gupta, J. J. Rodrigues, V. H. C. de Albuquerque, Dcavn: Cervical cancer prediction and classification using deep convolutional and variational autoencoder network, Multimedia Tools and Applications (2020) 1–17doi:<https://doi.org/10.1007/s11042-020-09607-w>.
- [50] A. Ghoneim, G. Muhammad, M. S. Hossain, Cervical cancer classification using convolutional neural networks and extreme learning machines, Future Gener. Comput. Syst. 102 (2020) 643–649. doi:<https://doi.org/10.1016/j.future.2019.09.015>.
- [51] M. M. Rahaman, C. Li, Y. Yao, F. Kulwa, X. Wu, X. Li, Q. Wang, Deepcervix: A deep learning-based framework for the classification of cervical cells using hybrid deep feature fusion techniques, Comput. Biol. Med. 136 (2021) 104649. doi:<https://doi.org/10.1016/j.compbiomed.2021.104649>.
- [52] J. Shi, R. Wang, Y. Zheng, Z. Jiang, H. Zhang, L. Yu, Cervical cell classification with graph convolutional network, Comput. Methods Programs Biomed. 198 (2021) 105807. doi:<https://doi.org/10.1016/j.cmpb.2020.105807>.
- [53] A. Manna, R. Kundu, D. Kaplun, A. Sinitca, R. Sarkar,

- A fuzzy rank-based ensemble of cnn models for classification of cervical cytology, *Sci. Rep.* 11 (1) (2021) 1–18. doi:<https://doi.org/10.1038/s41598-021-93783-8>.
- [54] A. R. Bhatt, A. Ganatra, K. Kotecha, Cervical cancer detection in pap smear whole slide images using convnet with transfer learning and progressive resizing, *PeerJ Comput. Sci.* 7 (2021) e348. doi:<https://doi.org/10.7717/peerj-cs.348>.
- [55] H. Basak, R. Kundu, S. Chakraborty, N. Das, Cervical cytology classification using pca & gwo enhanced deep features selection, arXiv preprint arXiv:2106.04919. URL <https://arxiv.org/abs/2106.04919>
- [56] J. Jantzen, J. Norup, G. Dounias, B. Bjerregaard, Pap-smear benchmark data for pattern classification, *Nature inspired Smart Information Systems (NiSIS 2005)* (2005) 1–9. URL <https://www.researchgate.net/publication/265873515>
- [57] Y. Xie, F. Xing, X. Kong, H. Su, L. Yang, Beyond classification: structured regression for robust cell detection using convolutional neural network, in: *International conference on medical image computing and computer-assisted intervention*, Springer, 2015, pp. 358–365. doi:https://doi.org/10.1007/978-3-319-24574-4_43.
- [58] P. Sukumar, R. Gnanamurthy, Computer aided detection of cervical cancer using pap smear images based on adaptive neuro fuzzy inference system classifier, *J. Med. Imaging Health Inf.* 6 (2) (2016) 312–319. doi:<https://doi.org/10.1166/jmih.2016.1690>.

Appendix

Table 12: A brief introduction to the deep learning models used in the robustness comparison experiment.

Model	Ref.	Parameters	Top-1 accuracy	Major remarks
VGG11	[23]	133M	69.02%	a.The network has deeper layers and uses smaller filters. b.Training takes a long time.
VGG13		133M	69.93%	
VGG16		138M	71.59%	
VGG19		144M	72.38%	
ResNet18	[24]	11.7M	69.76%	a.The residual block is introduced. b.The problem of rapid decline in accuracy due to the increase in the number of network layers is solved.
ResNet34		21.8M	73.31%	
ResNet50		25.6M	76.13%	
ResNet101		44.7M	77.37%	
DenseNet121	[25]	8M	74.43%	a.A direct connection between any two layers with the same feature map size is introduced. b.It can scale to hundreds of layers.
DenseNet169		14.3M	75.60%	
InceptionV3	[26]	23.8M	77.29%	a.It uses improved Inception Module. b.It introduces the idea of Factorization into small convolutions.
Xception	[27]	22.9M	79.00%	a.It is an improved version of InceptionV3. b.It uses depthwise separable convolutions.
AlexNet	[28]	60M	56.52%	a.ReLu activation function is introduced. b.The Local Response Normalization (LRN) layer is proposed to improve the generalization ability of the model.
GoogLeNet	[29]	6.8M	69.78%	a.It introduces the inception structure. b.It adopts multi-scale processing and Hebbian principle.
MobileNetV2	[30]	3.4M	71.89%	a.Inverted residual with linear bottleneck is introduced.
ShuffleNetV2×1.0	[31]	2.3M	69.36%	a.It uses channel split at the beginning of the block.
ShuffleNetV2×0.5		1.4M	60.55%	
InceptionResNetV1	[32]	8M	78.70%	a.It combines the Inception block and the ResNet connection.
ViT	[20]	86M	73.38%	a.It applies the Transformer to the field of computer vision. b.It is better than CNN under the training of a large amount of data.
BoTNet	[33]	20.8M	77.00%	a.It combines self-attention with ResNet.
DeiT	[34]	5M	72.20%	a.Distillation token is introduced. b.The training of DeiT requires less data and computing resources.
T2T-ViT	[35]	4.2M	71.70%	a.A new T2T mechanism based on ViT is used.